International Journal of Material Forming (2022) 15: 32
https://doi.org/10.1007/s12289-022-01688-2

ORIGINAL RESEARCH

Interfacial heat transfer coefficients in cold forging of stainless steel

Patrick Volke[1] · **Peter Groche**[1]

Received: 20 January 2022 / Accepted: 22 March 2022 / Published online: 6 April 2022

Abstract
In numerical simulations of cold forging processes, the heat transfer coefficient has a significant influence on the resulting temperature fields. However, the values determined so far for steel materials are not in the load range of cold forging processes. In this paper, a test stand for the determination of the interfacial heat transfer coefficient under typical loads of metal forming processes is presented. The results are discussed at an example of a cold extrusion forming process. It can be shown that the value increases significantly with increasing contact pressures and are higher compared to values known from literature. The investigations also disclose the influences of lubricants and the mechanical surface treatment on the heat transfer coefficient.

Keywords Interfacial heat transfer coefficient · Stainless steel · Cold forging

Introduction

Forming operations are highly efficient manufacturing processes which are known for their high material usage. Cold forging operation in particular also benefit from their ability to produce near net-shape components with superior material properties due to the occurring cold hardening effect. These advantageous characteristics can primarily be related to the plastic deformation of semi-finished products at room temperature. However, the forming at room temperature also entails some challenges since high tribological loads may occur during the forming process. Contact normal stresses can reach values around 3000 MPa [1, 2], locally distributed surface enlargements may reach up to 30 [3] and the relative velocity between the tool and workpiece can reach values up to 500 mm/s [4]. Due to the transformation of forming and friction energy into heat, it is reported that the average tool temperature can reach values of 200 °C [2]. In the tool/workpiece interface local spike temperatures may be even higher in a range between 500 and 600 °C [1, 2].

Complex lubricant systems are used to withstand these tribological loads. These are intended to separate the materials and tools from each other during forming in order to reduce friction and the required forming force on the one hand and to avoid possible tool wear on the other. In addition to oils and soaps in combination with conversion layers, ecologically advantageous single-layer lubricants based on molybdenum disulfide (MoS_2) and polymers have been increasingly used in recent years. However, the performance of these lubricants depends significantly on the contact temperature during the forming process [5, 6].

Temperature measurement directly in the process proves to be challenging. Due to the high contact normal stresses, conventional thermocouples can only be embedded in the tools at a distance of several millimeters from the surface [7, 8], which means that the temperature measurement only takes place with a time delay and temperature peaks cannot be determined. Here, the advantage of temperature determination in numerical simulations in the form of time and spatially resolved temperature curves as well as the possibility of an exact design of future processes to specific temperature ranges and lubricant systems becomes apparent. However, the accuracy of the resulting temperatures depends, among other things, on the choice of the heat transfer coefficient. Analyses by Zang for a tribometer test for cold forging show that the change in the heat transfer coefficient results in a temperature difference of 90 °C [9]. Polozine and Schaeffer [10] investigated the influence of the inaccuracy of the heat

✉ Patrick Volke
volke@ptu.tu-darmstadt.de

Peter Groche
groche@ptu.tu-darmstadt.de

[1] Institute for Production Engineering and Forming Machines, Technische Universität Darmstadt, Darmstadt, Germany

transfer coefficient in the simulation of open and closed die forging processes for aluminum and steel materials. They conclude that temperature errors of a few tenths to several hundred degrees Celsius can occur with the incorrect choice of the heat transfer coefficient and that it occurs more clearly at low initial sample temperatures.

Literature values for the heat transfer coefficient in the field of solid forming are not well documented. Bonnavand et al. [11] cite heat transfer coefficients in the range of 8000–20,000 W/(m^{2}K) for a simulation of cup-back extrusion. General values for stainless steel based on experimental determinations are in a similar range of 12,000–18,000 W/(m^{2}K) for contact pressures of 5–150 MPa [12–15].

The heat transfer coefficient describes the heat transfer from non-ideal surfaces, which have a lower thermal conductivity due to air pockets between surface asperities. Here, the influences of geometric, mechanical as well as thermal factors can be summarized [16]. Various studies have shown that the types of contact and intermediate materials, temperature, contact pressure as well as surface roughness have an influence on the heat transfer coefficient [12–14, 17, 18]. The contact pressure is shown to be a significant influencing parameter, an increase leads to a non-linear increase of the heat transfer coefficient [12]. The reason can be found in the elastic and plastic flattening of the surface structure, which results in an increase in the total effective contact area [19]. The influence of the intermediate material on the heat transfer coefficient depends on the thermal properties (heat conduction) of the material [20]. Intermediates such as MoS_2 and graphite based lubricants can reduce the heat transfer coefficient as heat conduction is lower compared to air [17, 18, 20]. However, a layer that is too thick has the opposite effect [21].

In summary, the temperature determination with simulations has advantages but is still prone to errors due to wrongly selected heat transfer coefficients. Current literature values with contact pressures of max. 150 MPa compared to the possible pressures of up to 3000 MPa are subject to uncertainties. The influences of the lubricants used in cold forging are also not taken into account.

The aim of this paper is to investigate the heat transfer coefficient for the load collective of cold forging. In addition to the influence of contact pressures above the yield stress, the lubricant systems used in cold forging and different surface topographies are investigated.

An experimental test rig has been developed to determine the heat transfer coefficients at high contact pressures. The experimental setup is explained below. After describing the evaluation methodology, the results are presented and the influences of the different test parameters are shown and discussed.

Test rig and setup

The test rig for determining the heat transfer coefficient is based on the experimentally steady state method with two punches and one sample according to Rosochowska et al. [22]. The schematic test setup is shown in Fig. 1. Due to the design with two punches made of tool steel (1.2379 / AISI D2) hardened to 58 HRC, contact normal stresses above the yield point of the sample material can be realized. The test has been designed for the press of the sliding compression test [23], which, due to its use as a tribometer for hot forging, has the necessary requirements for the temperatures and forces that occur in the tests. The test setup consists of a heater in the lower area, two cylindrical punches made of hardened tool steel, a specimen and cooling in the upper area. The entire experimental set-up is thermally insulated from the environment, inside the force path with pressure-resistant insulation materials and around the specimen and punches with a contacting flexible insulator based on glass wool. The lower die is embedded on the press table with the heater. During the test, the normal force is applied via the upper punch and kept constant for the test duration of 300 s. Figure 1 shows the temperature curve over the eight

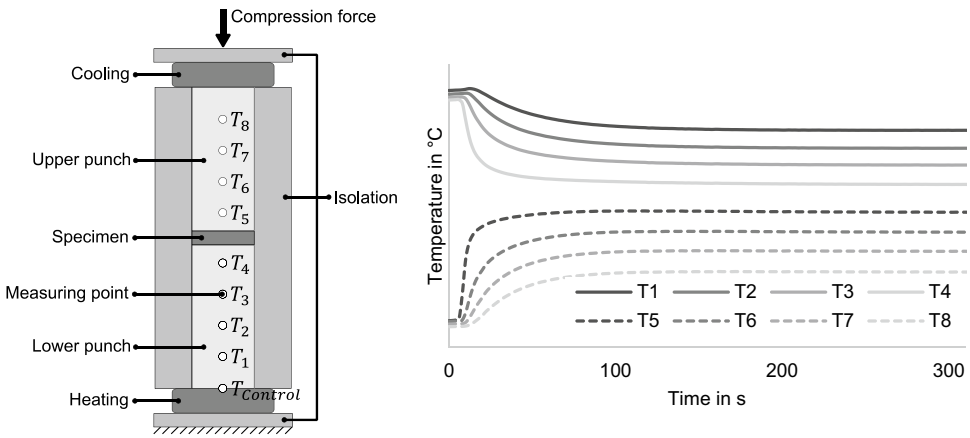

Fig. 1 Schematic illustration of test rig and temperature curve over the 8 measuring points during the test

measuring points inside the ram. As soon as the upper punch comes into contact with the specimen, temperature equalization begins in the system until a thermally steady state has been reached in the punches and the specimen and the temperatures remain constant.

The cylindrical specimens are made of the austenitic stainless steel 1.4404 (AISI 316 L) frequently used in the screw industry with a diameter of 18 mm and a height of 2 mm. The variable test factors are varied in the form of the upsetting force (4 variations), the control temperature (2 variations), the specimen surface (2 variations) and the intermediate material (3 variations). For each parameter variation, the test is repeated with three samples. Table 1 gives an overview of the test parameters.

The two control temperatures $T_{Control}$ of 300 °C and 400 °C, which are measured between the heater and the lower punch, result in extrapolated mean specimen temperatures of around 152 °C and 206 °C respectively. The sample surface is examined in both the blasted (Sq = 3.2 µm) and ground (Sq = 0.2 µm) condition. The blasted surface reflects the condition for industrial use. For the intermediate materials, two single-layer lubricants based on MoS_2 and polymers are used. The samples are coated with the lubricant in an immersion bath according to the manufacturer's specifications. In the bath, the lubricant is mixed with water in a ratio of 1:1.

Table 1 Test parameters for investigating the influences on the heat transfer coefficient

Test parameters				
Upsetting force	100 kN	150 kN	200 kN	250 kN
Control temperature	300 °C	400 °C		
Specimen surface	Blasted	Ground		
Intermediate material	MoS_2	Polymer	–	

The dried lubricant on the sample has a layer weight of approximately 15 g/m^2, which is typical for cold forging. As a reference, the tests are also carried out without an intermediate material. The fourth influencing parameter, the contact normal stress, is set via the upsetting force as a controllable parameter of the press in four stages from 100 kN to 250 kN. When using the two lubricants as an intermediate material, the coefficient of friction between the specimen and the die is reduced, which leads to a deformation of the specimen starting from an upsetting force of 150 kN and results in slightly different contact normal stresses compared to the reference without lubricant. Figure 2 shows the difference in contact normal stress for the two cases of different friction conditions over the four force levels. The determination of the contact pressure over the specimen radius is the result of a numerical simulation of the compression process of the specimen between the two punches at the four forces. Based on tribometer tests of the two lubricants with a coefficient of friction of µ = 0.03 (polymer lubricant) and µ = 0.07 (MoS_2 lubricant), an average coefficient of friction of µ = 0.05 is used for the simulation of the tests with a lubricant as intermediate material. By varying the friction coefficient in the simulation and comparing it with the real specimen geometry, a friction coefficient of µ = 0.45 is selected for the simulation of the tests without intermediate material.

With a compression force of 100 kN, there is no difference in the curve of the two friction coefficients and the contact pressure is constant over the specimen radius. Starting from an upsetting force of 150 kN, the curves of the contact pressure over the radius deviate between the two coefficients of friction. For the coefficient of friction µ = 0.45, the curve is largely constant over the radius until it drops towards the edge. In comparison, with a coefficient of friction of µ = 0.05, the contact pressure drops

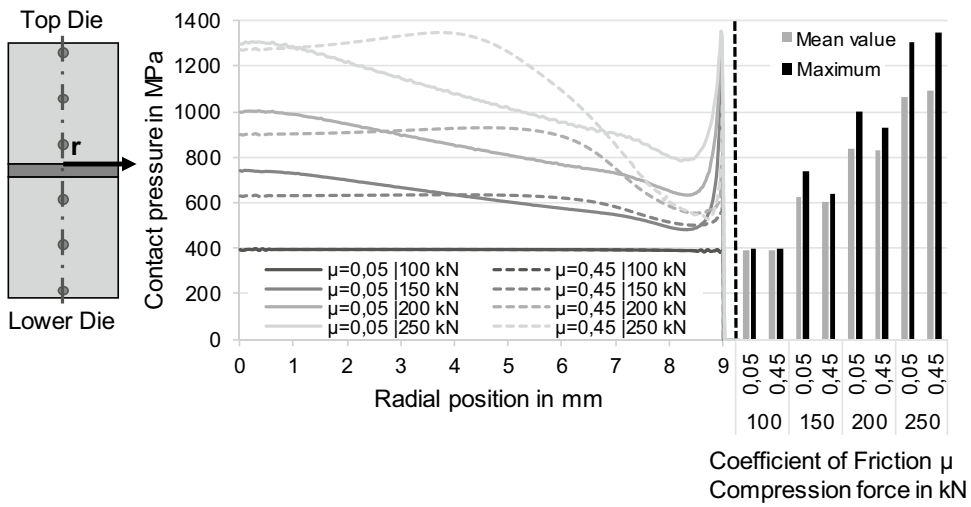

Fig. 2 Course of contact pressure over the sample radius for two friction values and four force levels

evenly from the maximum in the center of the sample towards the edge. When comparing the values of the contact pressures for the two friction coefficients, a difference of 40–105 MPa occur at the maximum. In addition, the arithmetic mean value of the contact pressure over the specimen radius is calculated based on the simulation results. The mean value reduces the difference to just 10–30 MPa, which makes the tests with and without lubricant comparable.

The difference in contact pressure is also reflected in the equivalent stress. At an upsetting force of 100 kN, the equivalent stress for both friction coefficients is 391 MPa over the specimen radius. At 150 kN, the equivalent stress for the case without lubricant is 422 MPa. With the friction coefficient of $\mu = 0.05$, the equivalent stress increases from 421 MPa at the specimen center to 485 MPa toward the specimen rim. With a yield stress of 440 MPa of the test material, the plastic deformation of the specimen begins. This results in a reduction of the height of the specimen and an increase of the diameter starting at an upsetting force of 150 kN (Fig. 3). The specimen without intermediate material ($\mu = 0.45$) shows only negligible deformation under load. At the maximum load of 250 kN, this is reflected in an increase of the radius of only 0.05 mm compared to the radial increase of 1 mm of the specimen with a coefficient of friction of $\mu = 0.05$. Due to the flexible radial insulation, the insulation effect is still maintained at the maximum radial enlargement of the specimen by 1 mm.

In the thermally steady state of the test stand, the temperature distribution across the bodies is constant. Together with the assumption of one-dimensional heat flow, the heat flow through the touching bodies is also constant. If the temperature of the measuring points is known, the heat transfer coefficient can be derived by linear extrapolation and Fourier's law. This method of calculating the heat transfer coefficient for the experimentally steady-state test is already well documented in the literature [15, 17, 22]. The only difference in the setup with two punches and one sample is that there are two heat transfers during the experiment due to the two contact surfaces between the punches and the sample, which means that the calculated heat transfer coefficient is the average over both contact surfaces.

Results and discussion

Figure 4 shows the plot of the heat transfer coefficient for the ground and blasted specimen without an intermediate for both temperatures 300 °C and 400 °C at an increasing average contact pressure of 389–1095 MPa. In addition, literature values for stainless steels are added to the diagram. Compared to the literature values, already an increase in

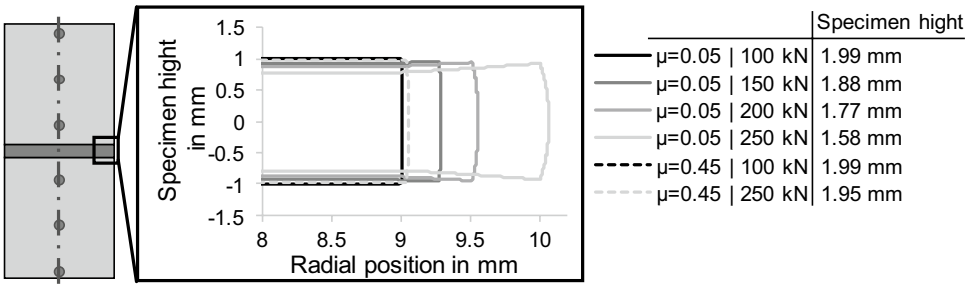

Fig. 3 Specimen height in relation to contact pressure at $\mu = 0.05$

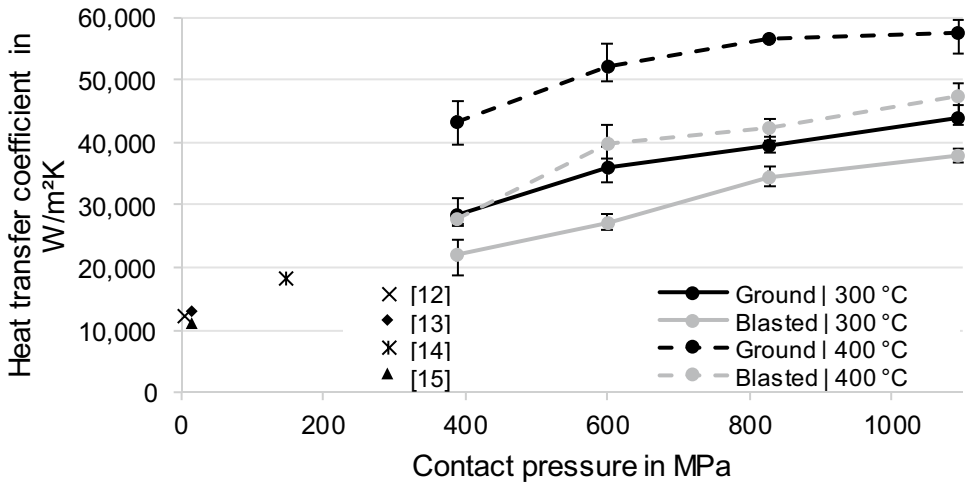

Fig. 4 Development of the heat transfer coefficient over the contact pressure for blasted and ground surfaces at 300 °C and 400 °C in comparison with four literature values

the heat transfer coefficient for higher contact pressures and can be seen. This trend continues as the load is increased up to 1095 MPa. For the tests at 300 °C, this results in an increase in the heat transfer coefficient of 55% for the ground and 73% for the blasted test samples. The influence of the surface is particularly evident at the lower contact pressures (389 MPa and 601 MPa). There, the heat transfer coefficient of the ground sample is about 30% higher than that of the blasted sample. With increasing contact pressure, this difference diminishes to 15%.

The increase of the temperature to 400 °C results in an increase of the heat transfer coefficient by 43% on average for the ground surface and by 31% for the blasted samples. Also evident is the greater increase in the coefficient for the blasted surface (71%) compared to the ground sample (33%).

An explanation for the differences between the two surfaces and the contact pressure can be found in the surface topographies. For that purpose, the center of the specimen is measured by means of a confocal microscope. This area, measuring 4.65 × 1.34 mm, has the highest contact pressures on the specimen. Figure 5 shows the overview of the surface parameters for the two initial surfaces versus the contact pressure for a temperature of 300 °C. For this purpose, 4 surface parameters according to DIN EN ISO 25178-2 are considered. For a general classification the mean square height Sq is used. In order to be able to describe the change of the surface better, the three function parameters Sk, Spk and Svk are used. The three parameters divide the topography in three areas (peak, core and sink) and allow the characterization of highly stressed functional surfaces [24]. The reduced peak height Spk and the reduced sink depth Svk describe the average height of the peaks as well as the average depth of the sinks with respect to the core area of the surface. This core area is defined by the core height Sk.

The mean square height Sq gives a first impression of the average surface height. For the blasted specimen, mean square height ranges from Sq = 3.2 µm at baseline to Sq = 2.15 µm at contact pressures 828 MPa and 1095 MPa. The reduced sink depth Svk, ranges around Svk = 4 µm for all loads within the scatter bars, indicating that the valleys are not affected by the simple compressive loading. The majority of the peaks of the surface are significantly leveled at the first load, which is reflected in the reduced peak height Spk. This decreases from Spk = 3.4 µm in the initial state to Spk = 0.9 µm at a contact pressure of 389 MPa and Spk = 0.5 µm (1095 MPa). The core height Sk, in combination with the reduced peak height Spk, is a good indicator of the leveling of the surface with increasing load. At the first load (389 MPa), the core height Sk = 7.4 µm remains unchanged compared to the initial condition, indicating that only the tips of the surface are leveled at this load as described earlier. As the load increases, the core height continuously decreases to Sk = 3.4 µm at 1095 MPa. Thus, with the core height and reduced peak height, a change can be detected even at the loads of 828 MPa and 1095 MPa, which is not present with the mean square height Sq.

The ground surface is more compact with Sq = 0.20 µm compared to the blasted specimen (Sq = 3.21 µm) and is also not as clearly leveled at the maximum load (Sq = 0.10 µm at 1095 MPa). This difference is also evident in the structure of the surface and the behavior of the peaks and valleys under loading. In the initial state, the reduced peak height is Spk = 0.15 µm, and the reduced valley depth is almost twice as large, Svk = 0.27 µm, giving the surface an asymmetric structure of the height density curve compared to the blasted sample. Under loading, the surface also behaves differently during leveling compared to the blasted specimens. The reduced peak height is constant over the four loads, hovering around Spk = 0.10 µm. With increasing load, the characteristics of the core height decrease from Sk = 0.49 µm to Sk = 0.22 µm as well as the reduced sink depth from Svk = 0.27 µm to Svk = 0.13 µm.

The already described increasing course of the heat transfer coefficient (Fig. 4) is accompanied by a reduction of the surface roughness for both surface topographies.

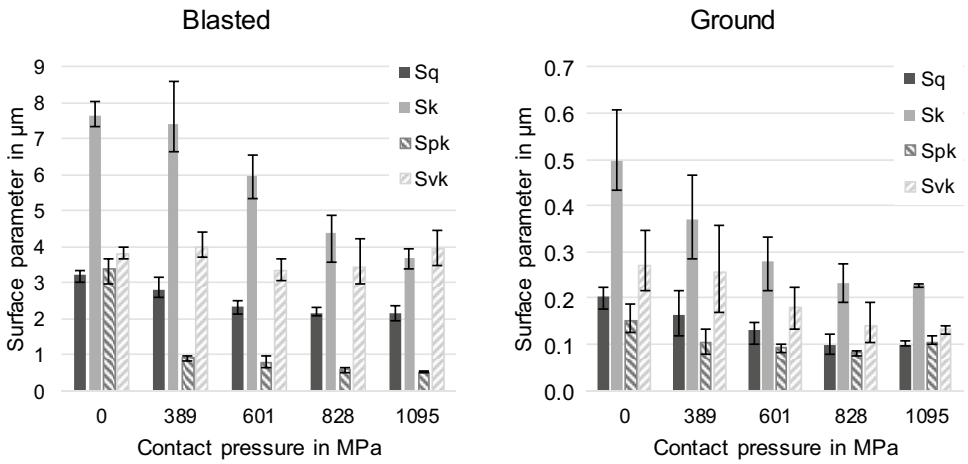

Fig. 5 Surface characteristics for blasted and ground specimens without lubricant at 300 °C

The reduction in the difference in heat transfer coefficient from 30% (389 MPa and 601 MPa) to 15% (828 MPa and 1095 MPa) between the two surface topographies can also be explained by the leveling of the surface. The ground surface shows a greater percentage leveling than the blasted surface at the contact pressures (389 MPa and 601 MPa). The surface roughness of the punches is with Sq = 0.02 significantly lower. The increase in the heat transfer coefficient can be explained with the increase in the real contact area between the rough specimen surface and the comparatively flat punch surface. This is particularly evident for the blasted surface, where the functional parameter Spk is reduced as the contact pressure increases. The reduction of this function parameter indicates the leveling of the surface peaks, which results in an increase of the contact to the flat punch surface.

The tests with the two single-layer lubricants based on MoS_2 and polymers are carried out at a temperature of 300 °C for both the ground and blasted samples. For the two low contact pressures, the heat transfer coefficients for the ground with and without a lubricant are similar (Fig. 6). A further increase in contact pressure results in a greater increase for the samples with the lubricants and ends in a nearly 20% higher heat transfer coefficient compared to the specimen without lubricant. The surface topography indicates that the increase is not due to a greater deformation of the surface.

Figure 7 shows the surface roughness of lubricant cleaned specimens in terms of mean square height Sq. Starting at the lowest load, the roughness of the specimens is still close to each other. As the contact pressure increases, the surface roughness of the specimen with the MoS_2 lubricant remains relatively constant. In comparison, the roughness of the polymer lubricant increases significantly, showing a 500% increase in surface roughness at the highest contact pressure.

The increase in roughness is due to the surface enlargement that occurs due to the lower friction of the polymer lubricant (μ=0,03 for the polymer lubricant and μ=0,07 for the MoS_2 lubricant). Wu et al. were already

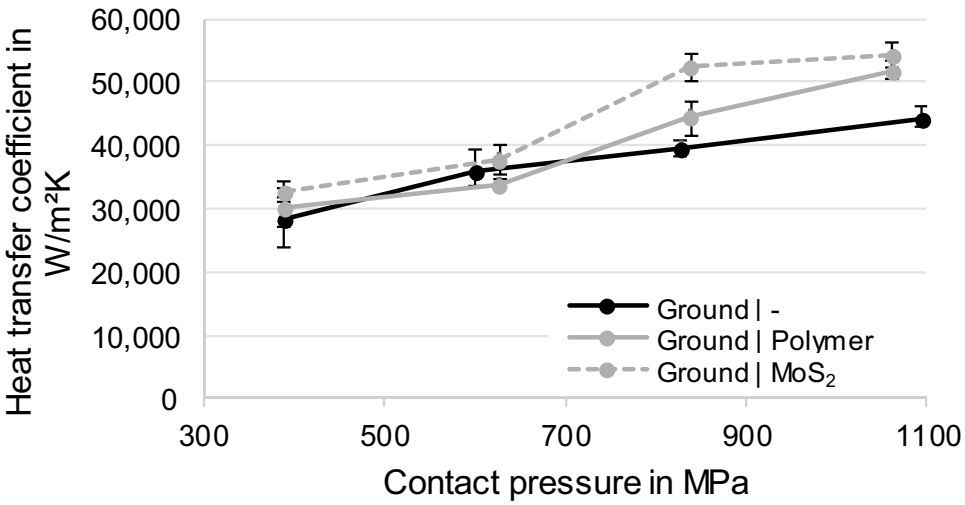

Fig. 6 Heat transfer coefficients versus contact pressure for ground specimens with and without additional lubricant at 300 °C

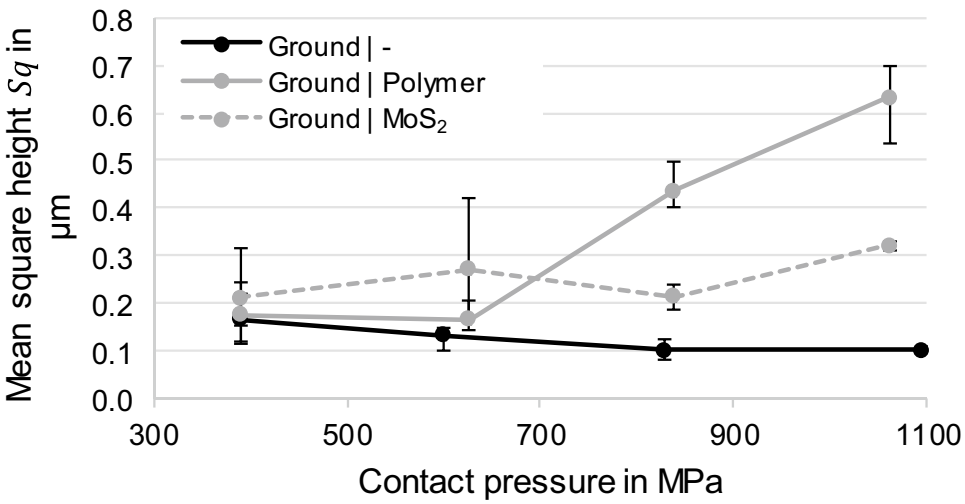

Fig. 7 Mean square height Sq versus contact pressure for ground specimens with and without additional lubricant

able to demonstrate the relationship between the surface strain and the increase in surface roughness in sheet metal forming, where the surface roughness of the sheet metal is in the range of the ground specimens [25]. The difference in the roughness increase can be explained by the different functioning principles of the polymer and MoS2 lubricants. The lubrication properties of the solid lubricant MoS2 are based on the molecular structure with a hexagonal lattice structure. The sliding planes connected by sulfur bridges can be shifted against each other under pressure [26]. The lubricating effect of the polymer lubricant is related to the temperature-viscosity behavior, which shows a significant reduction in lubricant viscosity above temperatures of 100 °C [9]. This low viscosity property of the polymer lubricant causes a lower resistance to surface deformation, which leads to an increase in roughness.

The lubricant embeds itself in the asperities of the surface topography and, due to the higher heat conduction compared to air, achieves an overall higher heat transfer coefficient and can thus also compensate for a rougher surface structure.

When lubricants are used in combination with the blasted surface, an approximately 20% higher heat transfer coefficient is shown compared to the reference without lubricant. For the highest contact pressure, this ratio increases to 56% for the MoS_2 lubricant (Fig. 8).

Compared to the ground specimens, the specimen surface of the blasted specimens behaves as known from the literature with a leveling of the surface (Fig. 9). This is even more pronounced for the specimens with lubricant, which can be explained by the easier deformation of the roughness peaks due to the reduced friction.

Summary and conclusion

After considering the heat transfer coefficients currently available in the literature for the simulation of cold forging processes as well as the general values and the contact pressures under which they are

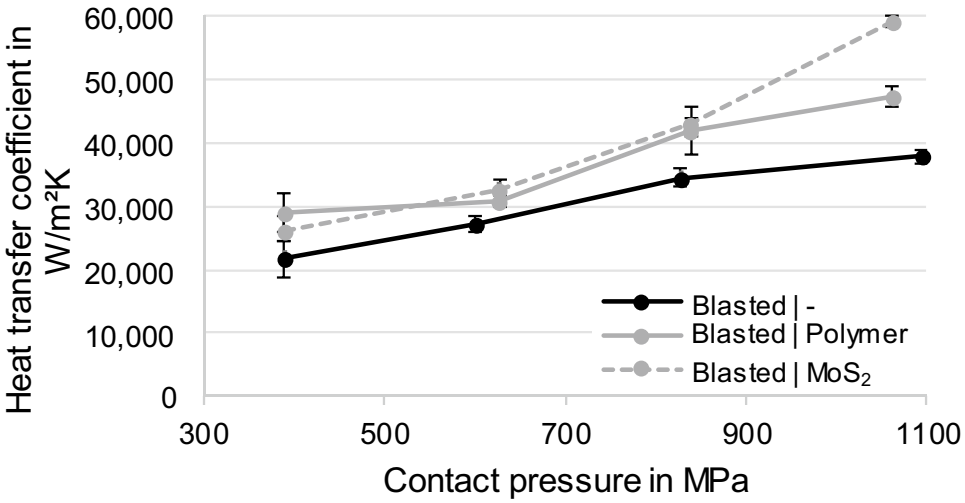

Fig. 8 Heat transfer coefficients versus contact pressure for blasted specimens with and without additional lubricant at 300 °C

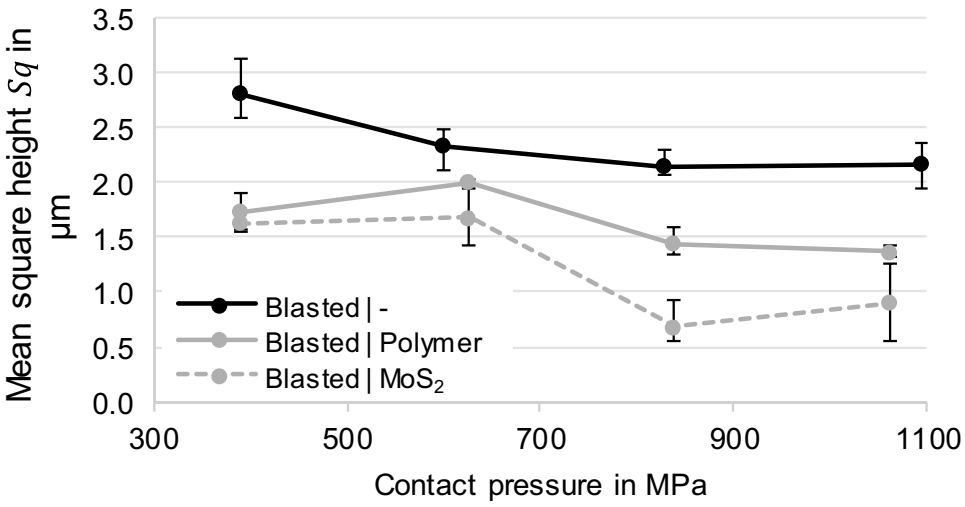

Fig. 9 Mean square height Sq versus contact pressure for blasted specimens with and without additional lubricant

recorded, an experimental setup is presented to determine the heat transfer coefficients at the process loads of cold forging. For the tests, the heat transfer coefficients are determined by varying the contact pressure, temperature, surface topography and lubricants. The results show that the heat transfer coefficients previously assumed in the literature for the loads of cold forging are significantly underestimated. For contact pressures around 1100 MPa, they range between h=47,000 W/m^{2}K and h=59,000 W/m^{2}K for the industrially relevant sample condition (blasted surface with a lubricant) depending on the lubricant used. Also, the results show that when lubricants are used, the surface condition has no significant influence on the heat transfer, since the lubricant fills the cavities created or present and can thus compensate for them.

Acknowledgements Results presented in this paper are achieved within the research project IGF 19803 N. Funding is provided by the German Federal Ministry of Economics and Energy via the German Federation of Industrial Cooperative Research Associations „Otto von Guericke "(AiF) in the program to encourage the industrial community research by an resolution of the German Bundestag and the Steel Forming Research Society (FSV). The long version of the final report can be ordered from the FSV, Goldene Pforte 1, 58093 Hagen.

Funding Open Access funding enabled and organized by Projekt DEAL.

Declarations

Competing interests The authors have no relevant financial or non-financial interests to disclose.

References

1. Bay N (1994) The state of the art in cold forging lubrication. J Mater Process Technol 46:19–40
2. Bay N, Azushima A, Groche P, Ishibashi I, Merklein M, Morishita M, Nakamura T, Schmid S, Yoshida M (2010) Environmentally benign tribo-systems for metal forming. CIRP Ann Manuf Technol 59:760–780
3. Steenberg T, Olsen JS, Christensen E, Bjerrum NJ (1999) Estimation of temperature in the lubricant film during cold forging of stainless steel based on studies of phase transformations in the film. Wear 232:140–144
4. Groche P, Müller C, Stahlmann J, Zang S (2013) Mechanical conditions in bulk metal forming tribometers—part one. Tribol Int 62:223–231
5. Groche P, Zang S, Müller C, Bodenmüller D (2015) A study on the performance of environmentally benign lubricants at elevated temperatures in bulk metal forming. J Manuf Process 20:425–430
6. Ludwig H, Zang S, Oehler O, Holz J, Ostowski J (2016) Umweltfreundliche Prozessketten in der Kaltmassivumformung von Abschnitten durch den Verzicht auf nasschemisch aufgebrachte Konversionsschichten. Abschlussbericht. Deutsche Bundesstiftung Umwelt (Projekt DBU 30738)
7. Doege E (2002) An innovative procedure for the numerical identification of accurate friction and heat transfer laws for precision forging processes. In: Goncalves R, Roy R, Steiger-Garcao A (Hrsg) Advances in Concurrent Engineering: Proceedings of the 9th ISPE International Conference on Concurrent Engineering, Cranfield, UK, 27–31 July 2002. Taylor & Francis
8. Müller C, Groche P (2014) Temperaturentstehung und die tribologischen Folgen bei Produktionsbeginn der Kaltmassivumformung. Schmiede Journal Nr. 09
9. Zang S (2017) Bestimmung von Temperaturen und deren Einflüsse auf tribologische Systeme der Kaltmassivumformung,Technische Universität Darmstadt. Dissertation
10. Polozine A, Schaeffer L (2008) Influence of the inaccuracy of thermal contact conductance coefficient on the weighted-mean temperature calculated for a forged blank. 3rd Braz Congr Manuf Eng 195:260–266
11. Bonnavand F, Bramley AN, Mynors DJ (2001) A fast new numerical tool for designing prestressed dies for backward extrusion: part 2: numerical analysis. In: proceedings of the institution of mechanical engineers. Part B: Journal of Engineering Manufacture 215:181–193
12. Singhal V, Litke PJ, Black AF, Garimella SV (2005) An experimentally validated thermo-mechanical model for the prediction of thermal contact conductance. Int J Heat Mass Transf 48:5446–5459
13. Tariq A, Asif M (2016) Experimental investigation of thermal contact conductance for nominally flat metallic contact. Heat Mass Transf 52:291–307
14. Burte PR, Im Y-T, Altan T, Semiatin SL (1990) Measurement and analysis of heat transfer and friction during hot forging. J Eng Ind 112:332–339
15. Dou R, Ge T, Liu X, Wen Z (2016) Effects of contact pressure, interface temperature, and surface roughness on thermal contact conductance between stainless steel surfaces under atmosphere condition. Int J Heat Mass Transf 94:156–163
16. Yovanovich MM (2005) Four decades of research on thermal contact, gap, and joint resistance in microelectronics. IEEE Transactions on Components and Packaging Technologies 28:182–206
17. Jain VK (1990) Determination of heat transfer coefficient for forging applications. J Mater Shap Technol 8:193–202
18. Zhu Z, Zhang L, Zhang C, Li R, Gu S (2016) Experimental investigation of transient contact heat transfer between 300M and 5CrNiMo. Int J Heat Mass Transf 96:451–457
19. Cooper MG, Mikic BB, Yovanovich MM (1969) Thermal contact conductance. Int J Heat Mass Transf 12:279–300
20. Liu X, Ji K, Fakir OE, Fang H, Gharbi MM, Wang L (2017) Determination of the interfacial heat transfer coefficient for a hot aluminium stamping process. 3rd Brazilian Congress on Manufacturing Engineering 247:158–170
21. Zhang XZ, Zhang LW, Xing L (2010) Study of thermal interfacial resistance between TC11/glass lubrication/K403 joint. Exp Thermal Fluid Sci 34:48–52
22. Rosochowska M, Chodnikiewicz K, Balendra R (2004) A new method of measuring thermal contact conductance. 3rd Braz Congr Manuf Eng 145:207–214
23. Groche P, Stahlmann J, Müller C (2013) Mechanical conditions in bulk metal forming tribometers—part two. Tribol Int 66:345–351
24. Volk R (2018) Rauheitsmessung: Theorie und Praxis. Beuth Verlag

25. Wu Y, Recklin V, Groche P (2021) Strain induced surface change in sheet metal forming: numerical prediction, influence on friction and tool Wear. JMMP 5:29
26. Mang T (2017) Forming lubricants. In: Dresel W, Mang T (Hrsg) Lubricants and lubrication. Wiley-VCH Verlag GmbH & Co. KGaA, Weinheim, pp. 639–780